MODELING, IDENTIFICATION AND COMPENSATION OF COMPLEX HYSTERETIC AND LOG(*t*)-TYPE CREEP NONLINEARITIES

K. Kuhnen

Laboratory for Process Automation (LPA), Saarland University,

Building 13, D-66123 Saarbrücken, Germany

e-mail: k.kuhnen@lpa.uni-saarland.de

Abstract

Undesired complex hysteretic nonlinearities and complex log(*t*)-type creep dynamics are present to varying degrees in virtually all smart-material based sensors and actuators provided that they are driven with sufficiently high amplitudes. In motion and active vibration control applications, for example, these nonlinearities can excite unwanted dynamics which leads in the best case to reduced closed-loop system performance and in the worst case to unstable closed-loop system operation. This necessitates the development of purely phenomenological models which characterize these types of nonlinearities and dynamics in a way which is sufficiently accurate, robust, amenable to control design for compensation and efficient enough for use in real-time applications. To fulfil these demanding requirements the present paper describes a new compensator design method for combined complex hysteretic nonlinearities and complex log(*t*)-type creep dynamics based on the so-called Prandtl-Ishlinskii approach. The underlying parameter identification problem which has to be solved to obtain a suitable compensator can be represented by a quadratic optimization problem which produces the best least-square approximation for the measured input-output data of the

real combined hysteretic nonlinearity and creep dynamics. Special linear inequality and equality constraints for the parameters guarantee the unique solvability of the identification problem, the invertability of the identified model and thus a reliable compensator design procedure. Finally the compensator design method is used to generate an inverse feedforward controller for the simultaneous compensation of the hysteretic nonlinearities and the log(*t*)-type creep dynamics of a piezoelectric stack actuator. In comparison with the conventionally controlled micropositioning stage with a nonlinearity error of about 14 % the inverse controlled micropositioning stage exhibits only about 1.7 % error.

Keywords

Hysteresis, Creep, Nonlinear Systems, Modeling, Identification, Compensation

1 Introduction

According to [1] a hysteretic nonlinearity is a rate-independent mapping between an input signal and an output signal with memory. This special property leads to the well-known rate-independent branching which can be observed in the input-output-plane of the system as illustrated in Fig. 1. Nearly all hysteretic nonlinearities in smart materials show further important characteristics in its branching behaviour which are summarized in the three Madelung rules [2]. In addition to these three Madelung rules a fourth important observation can be made for actuator and sensor characteristics of smart materials which is called the intersection property. Due to this property infinitely many branches can originate from a given point in the input-output-plane for a given direction of the input signal. A typical situation in which this property occurs is the intersection of different branches for the same direction of the input signal as indicated by the point *D* in Fig. 1a and Fig. 1b. The intersection effect can not be modeled by a local-memory hysteretic nonlinearity because it is characterized by a

scalar hysteretic state-variable which normally corresponds to the output variable. This simple memory structure allows only one branch for a given direction of the input signal.

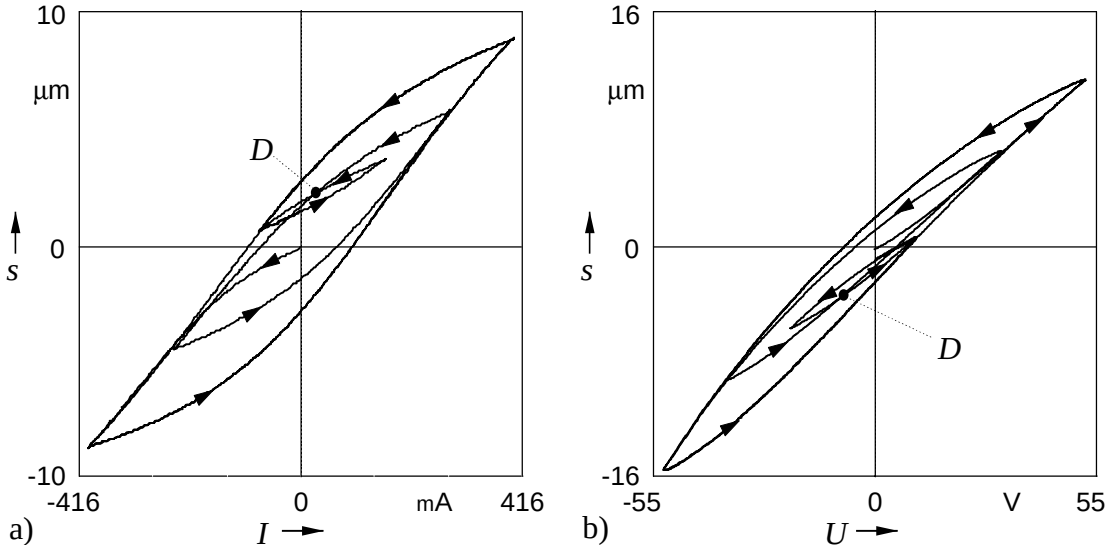

Figure 1. Complex hysteretic nonlinearities in smart material systems: a) measured current-displacement-characteristic of a magnetostrictive actuator b) measured voltage-displacement-characteristic of a piezoelectric actuator

For the modeling of hysteresis effects in smart material systems the corresponding hysteretic nonlinearity requires at least in principle an infinite dimensional memory representation and is therefore called a global-memory hysteretic nonlinearity [3]. The best-known examples of such systems are the Preisach and Prandtl-Ishlinskii operator which belong to the class of operators with a Preisach memory [4]. In numerical approximation schemes the infinite dimensional memory is often approximated by a finite but sufficiently high dimensional memory which according to [5] is called a complex memory. The best-known examples of these so-called complex hysteretic nonlinearities are the Krasnosel'skii-Pokrovskii operator and the threshold-discrete Prandtl-Ishlinskii operator which represents the finite dimensional approximations of the Preisach and Prandtl-Ishlinskii operators,respectively [6,7].

Memory-free and complex hysteretic nonlinearities are present in varying degree in virtually all smart-material based sensors and actuators provided that they are driven with sufficiently high amplitudes. The most familiar examples of complex hysteretic nonlinearities in smart-material systems are piezoelectric, electrostrictive, magnetostrictive and shape memory alloy based actuators and sensors [8]. In many cases, these types of nonlinearities can be limited through the choice of proper materials and operating regimes so that linear sensor and actuator characteristics can be assumed. But in the consequence of more stringent performance requirements a large number of systems are currently operated in regimes in which hysteretic nonlinearities are unavoidable.

Unfortunately, in addition to complex hysteretic nonlinearities, actuators and sensors based on the technologically important piezoelectric ceramics contain also log(t)-type creep dynamics to a degree which is not neglectable in wideband applications like micropositioning systems as shown in Fig. 2. The picture in the upper left part of Fig. 2 illustrates a typical measured input voltage signal U used in micropositioning applications as for example the atomic force microscopy [9] . This input voltage is a staircase function with small steps ΔU as shown in the encircled enlargement below the upper left picture. The corresponding measured displacement response s of the ceramic is shown in the upper right part of Fig. 2. The signal in the encircled enlargement below the upper right picture displays that part Δs of the displacement response which corresponds to the voltage step shown in the encircled enlargement below the upper left picture. Within the given time resolution of T_s = 1ms in this example the displacement response Δs consists of an immediate hysteretic part Δs_s and a time-delayed creep part Δs_d of approximately the same magnitude. The second encircled enlargment of this signal below displays this local step response Δs against the logarithmically transformed time axis $\log(\Delta t/T_s)$. In this diagram the creep part Δs_d is nearly linear with respect to the argument and is thus called log(t)-type creep.

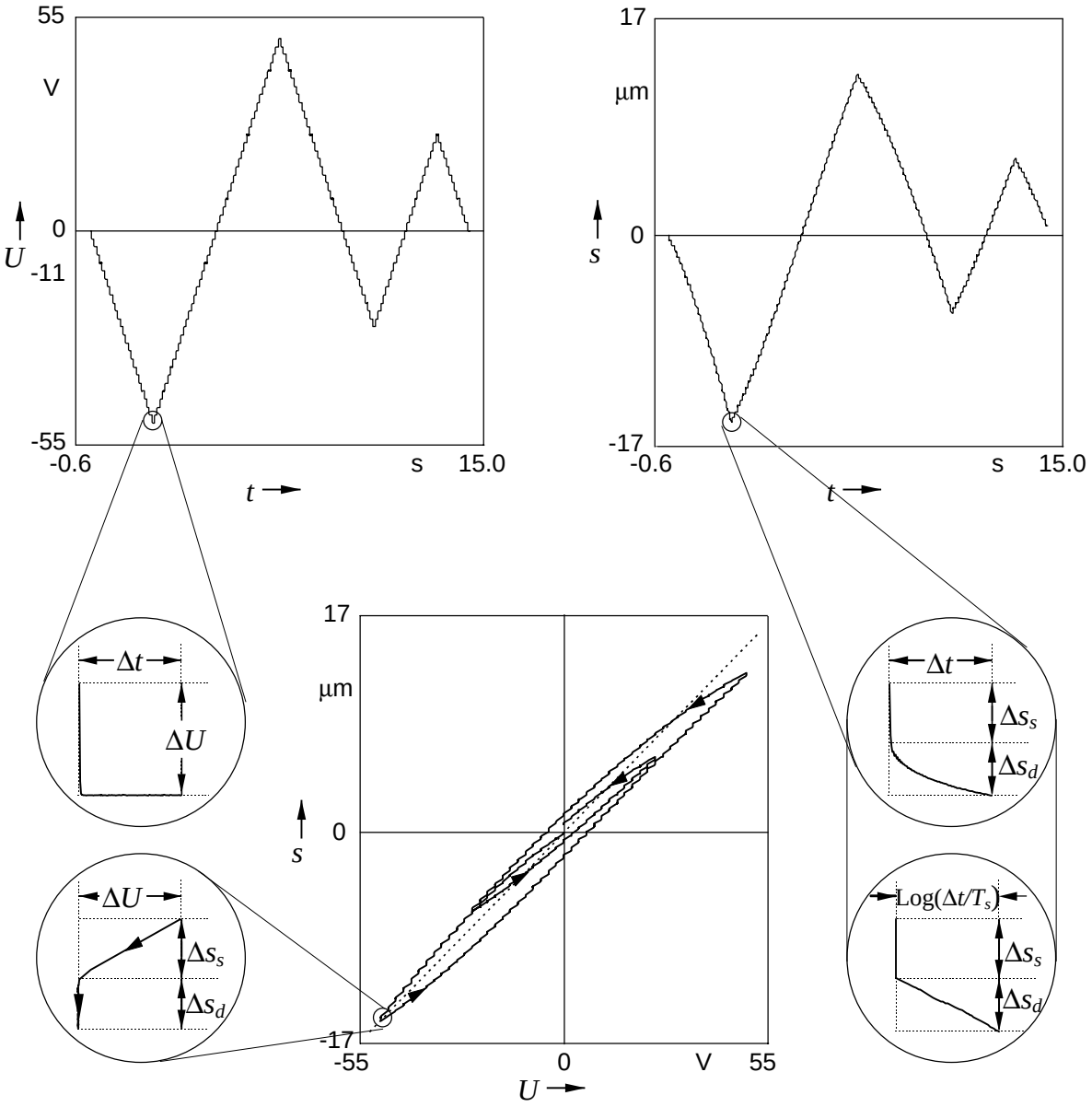

Figure 2. Voltage-displacement characteristic of a piezoelectric actuator as a combined complex hysteretic nonlinearity with log(t)-type creep dynamics.

As shown in the *U*-*s*-diagram in the lower middle of Fig. 2 and its corresponding encircled enlargement the immediate hysteretic part Δs_s generates diagonal and the time-delayed creep part Δs_d vertical segments in the *U*-*s*-trajectory. Moreover, this picture illustrates the hysteretic branching of the system and the existence of saturation effects which generate an asymmetrical major loop of the *U*-*s*-trajectory.

In motion and active vibration control applications, for example, these nonlinearities can excite unwanted dynamics which lead in the best case to reduced closed-loop system performance and in the worst case to unstable closed-loop system operation. This necessitates the development of purely phenomenological models that characterize these types of nonlinearities and dynamic effects in a way which is sufficiently accurate, amenable to compensator design for actuator or sensor linearisation and efficient enough for use in real-time applications.

Models of hysteretic nonlinearities have evolved from two different branches of physics: ferromagnetism and plasticity theory. The roots of both branches go back to the end of the 19th century. But only at the beginning of the 1970s was a mathematical formalism for a systematic consideration of hysteretic nonlinearities developed [5]. The core of this theory is formed by so-called hysteresis operators which describe hysteretic transducers as a mapping between function spaces. But it is only since the beginning of the 1990s that engineers employ this theory on a larger scale to develop modern strategies for the linearisation of hysteretic nonlinearities with an inverse feedforward controller, see Fig. 3.

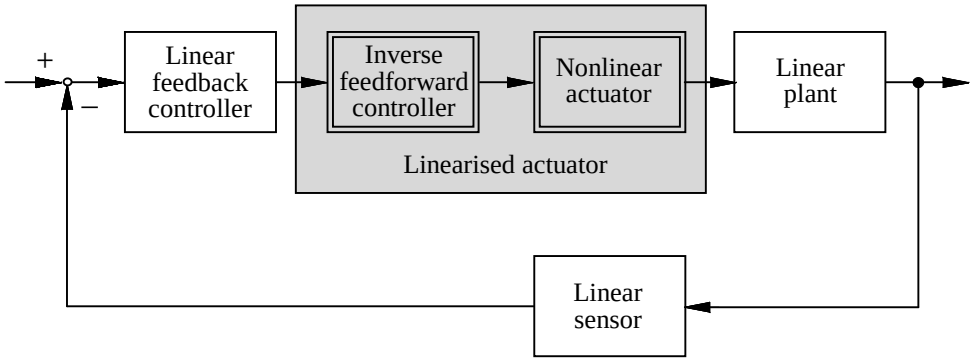

Figure 3. Linearisation of a hysteretic actuator by an inverse feedforward control strategy.

This type of controller is based on the compensator W^{-1} of the nonlinearity W which is defined as the operator fulfilling

$$W[W^{-1}[x]](t) = I[x](t)\,. \tag{1}$$

In (1) I is the Identity operator which describes the idealized transfer characteristic

$$I[x](t) = x(t)\,. \tag{2}$$

One reason for this is the increasing number of mechatronic applications in recent years which use new solid-state actuators based on magnetostrictive or piezoelectric material or shape memory alloys.

Whereas in the beginning mainly the well-known Preisach operator was used for the modeling and linearization of solid-state actuators with the inverse control approach [10,11], recent papers also reference the so-called Krasnosel'skii-Pokrovskii operator [6] and the so-called threshold-discrete Prandtl-Ishlinskii operator [12,13,14] which belong to an important subclass of the Preisach operator. In contrast to the Preisach and Krasnosel'skii-Pokrovskii hysteresis modelling approach, this subclass permits am analytical design of the compensator which is an excellent precondition for its use in real-time applications [7]. Unfortunately, the Prandtl-Ishlinskii modelling approach considers only complex hysteretic nonlinearities with an odd symmetrical major loop in the input-output-plane. In the so-called modified Prandtl-Ishlinskii approach this main drawback was removed through a concatenation of a Prandtl-Ishlinskii operator and an asymmetrical memory-free nonlinearity which models the deviation of the real hysteretic nonlinearity from the class of Prandtl-Ishlinskii operators [15]. Other well-known hysteresis compensation techniques use compensators based on models for local hysteretic nonlinearities [16,17,27]. But as mentioned before, these models are too simple in their memory structure to model the complex hysteretic nonlinearities in smart material systems in a sufficiently precise way.

Models for dynamic creep effects have mainly evolved from the viscoelasticity and viscoplasticity theory of solid mechanics [18] and from the phenomenological models based on simple mechanical elements describing the experimentally observed rheological behaviour of solids and fluids [19]. Although precise phenomenological models for creep with a log(t)-

type dynamic have been known for a long time, a new method which incorporates phenomenological hysteresis and creep models into a common compensation strategy was just recently presented [20,21]. Unfortunately, the underlying visco-elastic type creep model in [20,21] has a linear memory-free equilibrium characteristic. But in reality the equilibrium characteristic of the log(*t*)-type creep processes in piezoceramics are complex hysteretic in nature as shown in [22] and are therefore called complex log(*t*)-type creep processes. Therefore, according to the classification of material responses in [23] a consistent modeling of complex log(*t*)-type creep processes requires visco-plastic type creep models with a complex equilibrium hysteresis.

Due to this motivation the main contribution of the present paper is the extension of the modified Prandtl-Ishlinskii compensator design approach for complex hysteretic nonlinearities to handle systems with additionally occuring complex log(*t*)-type creep dynamics.

The paper is organized as follows: The second section summarises shortly the basics of the modified Prandtl-Ishlinskii modelling and compensation approach for complex hysteretic nonlinearities. In the third section this approach will be extended to model and compensate simultaneously complex hysteretic nonlinearities and complex log(*t*)-type creep dynamics. Finally, in the fourth section the compensator design method is used to generate an inverse feedforward controller for the simultaneous compensation of the complex hysteretic nonlinearities and the complex log(*t*)-type creep dynamics of a commercially available micropositioning stage based on a piezoelectric stack actuator.

2 The modified Prandtl-Ishlinskii approach

The modified Prandtl-Ishlinskii approach has been developed recently for the modeling, identification and compensation of asymmetrically complex hysteretic nonlinearities and is the starting point for the extensions presented in the next chapter. Here we only sumarise the

relevant basics of this approach without any proof. For further details we refer to the original literature [24,25,15].

2.1 Complex hysteresis modeling

The modified Prandtl-Ishlinskii hysteresis operator is defined as the concatenation

$$\Gamma[x](t) = S[H[x]](t) \tag{3}$$

of a Prandtl-Ishlinskii hysteresis operator H and a Prandtl-Ishlinskii superposition operator S which models the memory-free nonlinearity as shown in Fig.4.

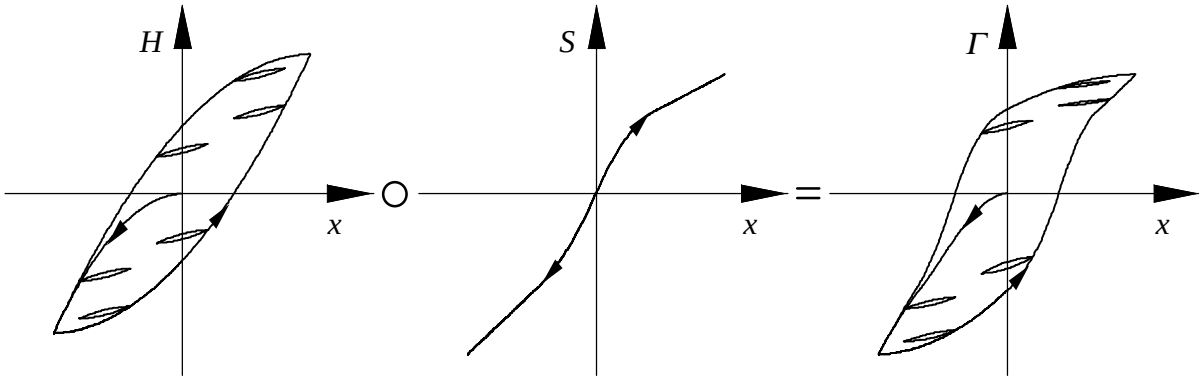

Figure 4. Modeling of asymmetrically complex hysteretic nonlinearities with a concatenation of H and S

As mentioned in the introduction the Prandtl-Ishlinskii hysteresis operator belongs to the class of operators with a Preisach memory which has a global memory structure [3]. The concatenation of this hysteresis operator with a memory-free nonlinearity according to (3) influences only the output mapping of the overall system and thus does not change this memory property. In practical applications we work with a finite dimensional approximation of this operator which is given in vector notation by

$$\Gamma[x](t) = \boldsymbol{w}_S^{\,T} \cdot \boldsymbol{S}_{\boldsymbol{r}_S}[\boldsymbol{w}_H^{\,T} \cdot \boldsymbol{H}_{\boldsymbol{r}_H}[x,\boldsymbol{z}_{H0}]](t)\,. \tag{4}$$

The operator H consists of a weighted linear superposition of n+1 elementary play operators H_{rH}, which are included in (4) in the n+1-dimensional vector $\boldsymbol{H}_{\boldsymbol{r}H}$. The rate-independent characteristic is characterised by the threshold-dependent x-y-trajectory (Fig. 5a). The weights

w_{Hi}, the thresholds r_{Hi} and the initial values z_{H0i}, $i = 0 \ldots n$ of the play operators are considered in the vector notation (4) by the vector of weights $\boldsymbol{w}_H{}^T = (w_{H0}\ w_{H1} \ldots w_{Hn})$, the vector of thresholds $\boldsymbol{r}_H{}^T = (r_{H0}\, r_{H1} \ldots r_{Hn})$ with $r_{H0} = 0$ and the vector of the initial values $\boldsymbol{z}_{H0}{}^T = (z_{H0}\ z_{H1} \ldots z_{Hn})$. The outputs of the elementary operators $z_{Hi} = H_{rH}[x,z_{H0i}]$, $i = 0 \ldots n$ represent the inner system state of the memory of the discrete-threshold Prandtl-Ishlinskii hysteresis operator.

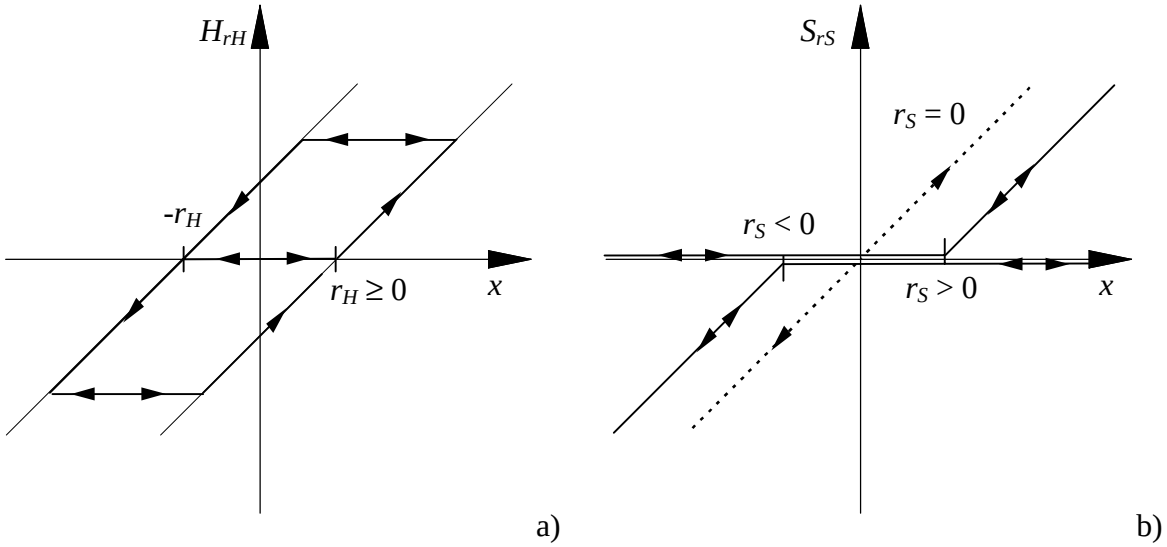

Figure 5. *x*-*y*-trajectory of the play (a) and the one-sided dead-zone operator (b).

The memoryless superposition operator *S* describes the deviation of the real characteristic from the odd symmetry property of the operator *H*. It consists of the weighted linear superposition of $2l+1$ one-sided dead-zone operators S_{rS}, which are included in (4) in the $2l+1$-dimensional vector $\boldsymbol{S}_{\boldsymbol{r}S}$. The rate-independent transfer characteristic is characterised by the threshold-dependent *x*-*y*-trajectory shown in Fig. 5b. The weights w_{Si} and the thresholds r_{Si}, $i = -l \ldots +l$ of the one-sided dead-zone operators are considered in the vector notation (4) by the vector of weights $\boldsymbol{w}_S{}^T = (w_{S-l} \ldots w_{S0} \ldots w_{Sl})$ and the vector of thresholds $\boldsymbol{r}_S{}^T = (r_{S-l} \ldots r_{S0} \ldots r_{Sl})$ with $r_{S0} = 0$.

2.2 Complex hysteresis compensation

As shown in detail in [24,15] the corresponding compensator

$$\Gamma^{-1}[y](t) = H^{-1}[S^{-1}[y]](t) = \boldsymbol{w}_H'^{\,T} \cdot \boldsymbol{H}_{\boldsymbol{r}_H'}[\boldsymbol{w}_S'^{\,T} \cdot \boldsymbol{S}_{\boldsymbol{r}_S'}[y], \boldsymbol{z}_{H0}'](t) \tag{5}$$

with $\boldsymbol{z}_{H0}$', $\boldsymbol{r}_H$', $\boldsymbol{w}_H$' $\in \Re^{n+1}$ and $\boldsymbol{r}_S$', $\boldsymbol{w}_S$' $\in \Re^{2l+1}$, which exists uniquely if the weights $\boldsymbol{w}_H$ and $\boldsymbol{w}_S$ fulfill the linear inequality constraints

$$\begin{pmatrix} \boldsymbol{U}_H & \boldsymbol{O} \\ \boldsymbol{O} & \boldsymbol{U}_S \end{pmatrix} \cdot \begin{pmatrix} \boldsymbol{w}_H \\ \boldsymbol{w}_S \end{pmatrix} - \begin{pmatrix} \boldsymbol{u}_H \\ \boldsymbol{u}_S \end{pmatrix} \geq \begin{pmatrix} \boldsymbol{o} \\ \boldsymbol{o} \end{pmatrix}, \tag{6}$$

follows from the inversion of H and S and the concatenation of S^{-1} and H^{-1}. The matrices and vectors in (6) are given by

$$\boldsymbol{U}_H = \begin{pmatrix} 1 & 0 & \cdots & 0 \\ 0 & 1 & \cdots & 0 \\ \vdots & \vdots & \ddots & \vdots \\ 0 & 0 & \cdots & 1 \end{pmatrix} \in \Re^{n+1 \times n+1},$$

$$\boldsymbol{U}_S = \begin{pmatrix} 1 & 1 & \cdots & 1 & \cdots & 0 & 0 \\ 0 & 1 & \cdots & 1 & \cdots & 0 & 0 \\ \vdots & \vdots & \ddots & \vdots & \iddots & \vdots & \vdots \\ 0 & 0 & \cdots & 1 & \cdots & 0 & 0 \\ \vdots & \vdots & \iddots & \vdots & \ddots & \vdots & \vdots \\ 0 & 0 & \cdots & 1 & \cdots & 1 & 0 \\ 0 & 0 & \cdots & 1 & \cdots & 1 & 1 \end{pmatrix} \in \Re^{2l+1 \times 2l+1},$$

$\boldsymbol{u}_H^{\,T} = (\varepsilon\ 0\ .\ .\ 0) \in \Re^{n+1}$ and $\boldsymbol{u}_S^{\,T} = (\varepsilon\ \varepsilon\ .\ .\ \varepsilon\ .\ .\ \varepsilon\ \varepsilon) \in \Re^{2l+1}$. $\boldsymbol{O}$ and $\boldsymbol{o}$ in (6) are matrices and vectors of zeros with corresponding dimensions. $\varepsilon > 0$ is a lower bound and a design parameter which permits the change of strict inequality contraints by the inequality constraints in (6).

According to (5) a main result of the Prandtl-Ishlinskii approach for the modeling of hysteresis and memory-free nonlinearities is the invariance property of the two model classes H and S with respect to the system inversion operation provided that condition (6) holds. As a consequence the inverses H^{-1} and S^{-1} have exactly the same model structure as the models H and S. The inverse filters differ from the models only in the values of the thresholds, the weights and the initial states if they are part of the system as in the case of the hysteresis

model. Between the thresholds, the weights and the initial states of the models and their corresponding inverses exist one to one correspondences which can be formulated as vector-valued transformation mappings [25]. That part of these mappings used in the following chapters is explicitly given by the formulas

$$\boldsymbol{w}'_H = \boldsymbol{\Phi}_H(\boldsymbol{w}_H) \triangleq \begin{cases} w'_{H0} = \dfrac{1}{w_{H0}} \\ w'_{Hi} = -\dfrac{w_{Hi}}{(w_{H0} + \sum_{j=1}^{i} w_{Hj})(w_{H0} + \sum_{j=1}^{i-1} w_{Hj})} \quad ; \quad i = 1 \,..\, n \end{cases} \tag{7}$$

$$\boldsymbol{r}'_H = \boldsymbol{\Psi}_H(\boldsymbol{r}_H, \boldsymbol{w}_H) \triangleq r'_{Hi} = \sum_{j=0}^{i} w_{Hj}(r_{Hi} - r_{Hj}) \quad ; \quad i = 0 \,..\, n\,, \tag{8}$$

$$\boldsymbol{z}'_{H0} = \boldsymbol{\Theta}_H(\boldsymbol{z}_{H0}, \boldsymbol{w}_H) \triangleq z'_{H0i} = \sum_{j=0}^{i} w_j z_{H0i} + \sum_{j=i+1}^{n} w_j z_{H0j} \quad ; \quad i = 0 \,..\, n\ , \tag{9}$$

$$\boldsymbol{w}_S = \boldsymbol{\Phi}_S(\boldsymbol{w}'_S) \triangleq \begin{cases} w_{Si} = -\dfrac{w'_{Si}}{(w'_{S0} + \sum_{j=i}^{-1} w'_{Sj})(w'_{S0} + \sum_{j=i+1}^{-1} w'_{Sj})} \quad ; \quad i = -l \,..\, -1 \\ w_{S0} = \dfrac{1}{w'_{S0}} \\ w_{Si} = -\dfrac{w'_{Si}}{(w'_{S0} + \sum_{j=1}^{i} w'_{Sj})(w'_{S0} + \sum_{j=1}^{i-1} w'_{Sj})} \quad ; \quad i = +1 \,..\, +l \end{cases} \tag{10}$$

$$\boldsymbol{r}_S = \boldsymbol{\Psi}_S(\boldsymbol{r}'_S, \boldsymbol{w}'_S) \triangleq \begin{cases} r_{Si} = \sum_{j=i}^{0} w'_{Sj}(r'_{Si} - r'_{Sj}) \quad ; \quad i = -l \,..\, 0 \\ r_{Si} = \sum_{j=0}^{i} w'_{Sj}(r'_{Si} - r'_{Sj}) \quad ; \quad i = 0 \,..\, +l \end{cases} \tag{11}$$

and transform a given model H to its inverse H^{-1} and a given inverse S^{-1} to the model S.

3 Complex log(t)-type creep extension

The term creep is used in the literature primarily in connection with the delayed deformation behavior of solid materials due to sudden mechanical loading [19]. Very similar behavior can

be observed to different degrees in the relationship between the respective physical parameters in ferromagnetic and ferroelectric materials as well as in magnetostrictive and - even more pronounced - in piezoelectric actuators. And so the term creep came to stand for more than just the delayed response between mechanical input and output parameters. It is not a far step then to go beyond the bounds of physics to obtain a purely phenomenological description of creep, which in this work will be achieved using the elegant operator based approach used to describe hysteresis. The complex log(*t*)-type creep effect shown in Figure 1 is representative of that observed in many of the technologically important piezoelectric ceramics and as such plays an important role in the field of solid-state actuation.

3.1 Complex log(*t*)-type creep modeling

An operator based model of complex log(*t*)-type creep will be achieved drawing from the approach to modeling hysteresis with the Prandtl-Ishlinskii hysteresis operator. The elementary creep operator

$$y(t) = K_{r_K a_K}[x, y_{K0}](t) \tag{12}$$

is introduced as the unique solution of the nonlinear differential equation

$$\frac{\mathrm{d}}{\mathrm{d}t} y(t) = a_K \max\{x(t) - y(t) - r_K, \min\{x(t) - y(t) + r_K, 0\}\} \tag{13}$$

with the initial condition

$$y(t_0) = y_{K0}\,. \tag{14}$$

The elementary creep operator is characterised fully by its threshold value $r_K \in \Re^+_0$ and its creep eigenvalue $a_K \in \Re^+$. Fig. 6a illustrates the step response of the elementary creep operator over the logarithmic time axis for various creep eigen values a_{Kj}.

In this case the creep eigenvalues are distributed exponentially over the reciprocal of time according to the equation

$$a_{Kj} = \frac{1}{10^{j-1} T_s} \quad ; \quad j = 1 \,..\, m \,. \tag{15}$$

T_S corresponds to the smallest integration interval, i.e. the time resolution or sampling period achievable in a practical application. This interval period is simultaneously the earliest possible point in time to observe the creep behaviour when one assumes a step-like excitation at time t_0 = 0 and an equidistant integration interval for calculating the creep process. An exponential distribution of the creep eigenvalues according to (15) and an unweighted summation of the elementary operators results in a creep operator which produces approximately a linear step response along the logarithmic time axis as shown in Fig. 6b. Therefore, the unweighted superposition of the elementary creep operators with creep eigenvalues according to (15) is called the log(t)-type creep operator.

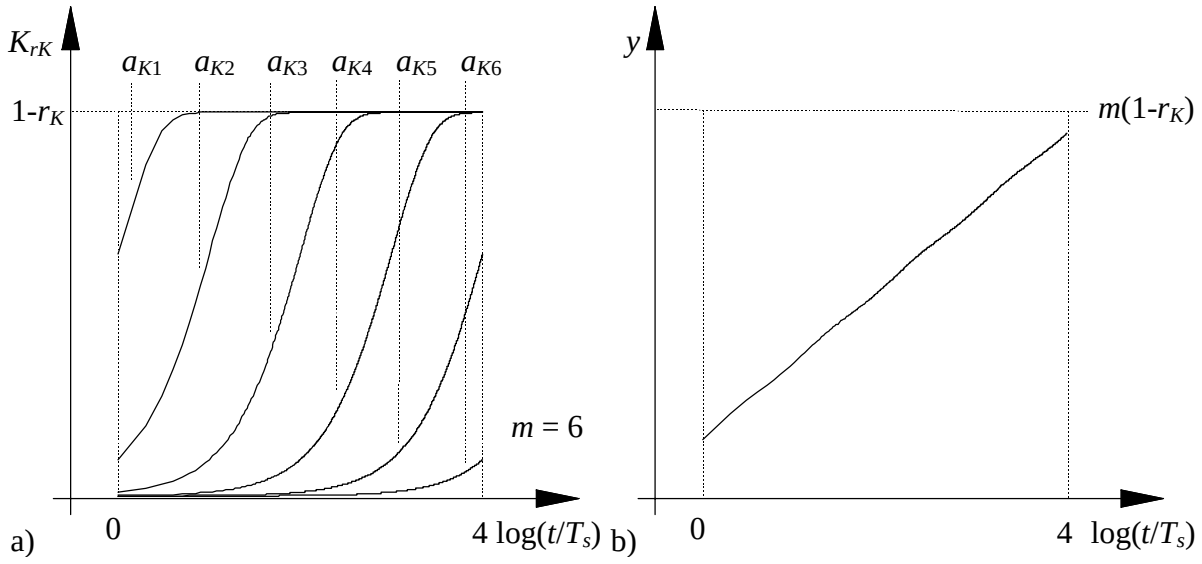

Figure 6. Step response of a) the elementary creep operator and b) a log(t)-type creep operator.

Considering the influence of the previous history of the input signal on the strength with which the log(t)-type creep is excited, results - analog to the Prandtl-Ishlinskii approach of modeling hysteresis - in several log(t)-type creep operators with various threshold values r_{Ki}. Thus, the Prandtl-Ishlinskii creep operator for complex log(t)-type creep effects is defined by

$$K[x](t) := \boldsymbol{w}_K^T \cdot \boldsymbol{K}_{\boldsymbol{r}_K \boldsymbol{a}_K}[x, \boldsymbol{Z}_{K0}](t) \cdot \boldsymbol{i}\,, \tag{16}$$

with the weight vector $\boldsymbol{w}_K{}^T = (w_{K0}\ w_{K1}\ .\ .\ w_{Kn})$, the threshold vector $\boldsymbol{r}_K{}^T = (r_{K0}\ r_{K1}\ .\ .\ r_{Kn})$ with $0 = r_{K0} < r_{K1} < .\ .\ < r_{Kn} < +\infty$, the creep eigenvalue vector $\boldsymbol{a}_K{}^T = (a_{K1}\ .\ .\ a_{Km})$, the matrix of initial conditions and the matrix of elementary creep operators

$$\boldsymbol{Z}_{K0} = \begin{pmatrix} z_{K001} & \cdots & z_{K00m} \\ z_{K011} & \cdots & z_{K01m} \\ \vdots & \ddots & \vdots \\ z_{K0n1} & \cdots & z_{K0nm} \end{pmatrix}, \quad \boldsymbol{K}_{\boldsymbol{r}_K \boldsymbol{a}_K}[x, \boldsymbol{Z}_{K0}] = \begin{pmatrix} K_{r_{K0} a_{K1}}[x, z_{K001}] & \cdots & K_{r_{K0} a_{Km}}[x, z_{K00m}] \\ K_{r_{K1} a_{K1}}[x, z_{K011}] & \cdots & K_{r_{K1} a_{Km}}[x, z_{K01m}] \\ \vdots & \ddots & \vdots \\ K_{r_{Kn} a_{K1}}[x, z_{K0n1}] & \cdots & K_{r_{Kn} a_{Km}}[x, z_{K0nm}] \end{pmatrix}$$

and the identity vector $\boldsymbol{i}^T = (1\ 1\ .\ .\ 1)$. According to this notation a log(t)-type creep operator with a threshold value r_{Ki} follows from the scalar multiplication of the corresponding row vector in the operator matrix $\boldsymbol{K}_{\boldsymbol{r}K\boldsymbol{a}K}$ with the identity vector $\boldsymbol{i}$. Thus, all log(t)-type creep operators with threshold value r_{Ki} , $i = 0\ .\ .\ n$ form a single column vector which is scalar multiplied with the weight vector $\boldsymbol{w}_K$ to obtain the Prandtl-Ishlinskii creep operator.

The operator K possesses a great structural similarity to the Prandtl-Ishlinskii hysteresis operator H which is recognizable in its asymptotic behavior for $\mathrm{d}x(t)/\mathrm{d}t \to 0$. According to [5] for $r_K = r_H$ and $y_{K0} = \max\{x(t_0) - r_K, \min\{x(t_0) + r_K, y_{H0}\}\}$ it follows

$$\lim_{a_K \to \infty} K_{r_K a_K}[x, y_{K0}](t) = H_{r_H}[x, y_{H0}](t)\,. \tag{17}$$

This means, that the elementary creep operator converges to the play operator for infinitely large creep eigenvalues or infinitely slow input signals. The immediate result for the Prandtl-Ishlinskii creep operator is the asymptotic behaviour

$$\lim_{\frac{\mathrm{d}}{\mathrm{d}t}x(t) \to 0} K[x](t) = H[x](t)\,, \tag{18}$$

where $\boldsymbol{w}_H = m \cdot \boldsymbol{w}_K$. Consequently, the Prandtl-Ishlinskii creep operator describes creep processes with log(t)-type creep dynamics and an equilibrium hysteresis of the Prandtl-Ishlinskii type. As such the introduced Prandtl-Ishlinskii creep operator can therefore be considered a dynamic generalization of the complex hysteresis operator H.

3.2 Complex hysteresis and log(*t*)-type creep modeling

The complete model for describing simultaneous hysteresis, log(*t*)-type creep as well as saturation processes results from the modified Prandtl-Ishlinskii hysteresis operator by adding the Prandtl-Ishlinskii creep operator to the Prandtl-Ishlinskii hysteresis operator. From this follows

$$\begin{aligned} \Gamma[x](t) &= S[H[x]+K[x]](t) \\ &= \boldsymbol{w}_S{}^T \cdot \boldsymbol{S}_{\boldsymbol{r}_S}[\boldsymbol{w}_H{}^T \cdot \boldsymbol{H}_{\boldsymbol{r}_H}[x,\boldsymbol{z}_{H0}]+\boldsymbol{w}_K{}^T \cdot \boldsymbol{K}_{\boldsymbol{r}_K\boldsymbol{a}_K}[x,\boldsymbol{Z}_{K0}]\cdot \boldsymbol{i}](t). \end{aligned} \tag{19}$$

In this extended model the Prandtl-Ishlinskii hysteresis operator can be considered as the component of the Prandtl-Ishlinskii creep operator with the creep eigenvalue $a_{K0} = \infty$. As such the hysteresis operator describes the component of creep that behaves as a complex hysteretic nonlinearity for the given input signal and time resolution. On the other hand under stationary operating conditions according to (18) the asymptotic behaviour is given by

$$\lim_{\frac{\mathrm{d}}{\mathrm{d}t}x\to 0} \Gamma[x](t) = \boldsymbol{w}_S{}^T \cdot \boldsymbol{S}_{\boldsymbol{r}_S}[\hat{\boldsymbol{w}}_H{}^T \cdot \boldsymbol{H}_{\boldsymbol{r}_H}[x,\boldsymbol{z}_{H0}]](t) \tag{20}$$

with $\hat{\boldsymbol{w}}_H = \boldsymbol{w}_H + m \cdot \boldsymbol{w}_K$. If the weights of the Prandtl-Ishlinskii creep operator obey the additional linear inequality contraints

$$\boldsymbol{U}_K \cdot \boldsymbol{w}_K - \boldsymbol{u}_K \geq \boldsymbol{o} \tag{21}$$

with the matrix $\boldsymbol{U}_K = \begin{pmatrix} 1 & 0 & \cdots & 0 \\ 0 & 1 & \cdots & 0 \\ \vdots & \vdots & \ddots & \vdots \\ 0 & 0 & \cdots & 1 \end{pmatrix}$ and the vector $\boldsymbol{u}_K = \begin{pmatrix} 0 \\ 0 \\ \vdots \\ 0 \end{pmatrix}$ the inequality constraints (6) are also fulfilled under stationary operating conditions.

3.3 Complex hysteresis and log(*t*)-type creep compensation

The inverse modified Prandtl-Ishlinskii creep and hysteresis operator Γ^{-1} which is necessary to compensate simultaneous occurrences of complex hysteresis, log(*t*)-type creep and staturation effects results from solving the implicit operator equation

$$
\begin{aligned}
x(t) &= H^{-1}[S^{-1}[y] - K[x]](t) \\
&= \boldsymbol{w}_H'^{\,T} \cdot \boldsymbol{H}_{\boldsymbol{r}_H'}[\boldsymbol{w}_S'^{\,T} \cdot \boldsymbol{S}_{\boldsymbol{r}_S'}[y] - \boldsymbol{w}_K^{\,T} \cdot \boldsymbol{K}_{\boldsymbol{r}_K \boldsymbol{a}_K}[x, \boldsymbol{Z}_{K0}] \cdot \boldsymbol{i}, \boldsymbol{z}_{H0}'](t).
\end{aligned} \tag{22}
$$

A suitable approach to solve the operator equation (22), which requires no more steps than the calculation of the operator Γ, can be derived analogue to the approach used in [21] and requires the inverse Prandtl-Ishlinskii hysteresis operator and the inverse Prandtl-Ishlinskii superposition operator in explicit form. These can be calculated explicitly up front from the operator Γ with the help of the transformation equations (7) - (11).

3.4 Complex hysteresis and log(*t*)-type creep identification

The starting point for the synthesis of the modified Prandtl-Ishlinskii hysteresis operator Γ and its compensator Γ^{-1} based on a given measured input signal $x(t)$ and its corresponding output signal $y(t)$ is the generalised error model

$$
\begin{aligned}
E[x,y](t) &= H[x](t) + K[x](t) - S^{-1}[y](t) \\
&= \boldsymbol{w}_H^{\,T} \cdot \boldsymbol{H}_{\boldsymbol{r}_H}[x, \boldsymbol{z}_{H0}](t) + \boldsymbol{w}_K^{T} \cdot \boldsymbol{K}_{\boldsymbol{r}_K \boldsymbol{a}_K}[x, \boldsymbol{Z}_{K0}](t) \cdot \boldsymbol{i} - \boldsymbol{w}_S'^{\,T} \cdot \boldsymbol{S}_{\boldsymbol{r}_S'}[y](t)
\end{aligned} \tag{23}
$$

which uses the models H and K and the inverse S^{-1}. Due to the use of the inverse S^{-1} instead of the model S we obtain an error model which depends linearly on the weights $\boldsymbol{w}_H$, $\boldsymbol{w}_K$ and $\boldsymbol{w}_S'$. As shown farther below this fact is of great importance for the practicability of the model and compensator synthesis procedure. On the other hand the dependence of this error model on the thresholds $\boldsymbol{r}_H$, $\boldsymbol{r}_K$ and $\boldsymbol{r}_S'$, the eigenvalues $\boldsymbol{a}_K$ and the initial states $\boldsymbol{z}_{H0}$ and $\boldsymbol{Z}_{K0}$ is nonlinear and this fact introduces some mathematical difficulties in the model and compensator synthesis procedure. Therefore, we try to determine these latter parameters from the properties of the measured input and output signal directly and then we regard them as given constants. With this idea in mind the synthesis of the modified Prandtl-Ishlinskii hysteresis operator Γ and its compensator Γ^{-1} is realised in three steps.

In the first step the thresholds $\boldsymbol{r}_H$, $\boldsymbol{r}_K$ and $\boldsymbol{r}_S'$, the eigenvalues $\boldsymbol{a}_K$ and the initial values $\boldsymbol{z}_{H0}$ and $\boldsymbol{Z}_{K0}$ are determined by the formulas (15),

$$r_{Hi} = \frac{i}{n+1} \max_{t_0 \le t \le t_e} \{|x(t)|\} \quad ; \quad i = 0 \,..\, n \,, \tag{24}$$

$$r_{Ki} = \frac{i}{n+1} \max_{t_0 \le t \le t_e} \{|x(t)|\} \quad ; \quad i = 0 \,..\, n \tag{25}$$

$$\begin{aligned} r'_{Si} &= \frac{(i+\frac{1}{2})}{l} \min_{t_0 \le t \le t_e} \{y(t)\} \quad ; \quad i = -l \,..\, -1 \\ r'_{S0} &= 0 \\ r'_{Si} &= \frac{(i-\frac{1}{2})}{l} \max_{t_0 \le t \le t_e} \{y(t)\} \quad ; \quad i = +1 \,..\, +l \end{aligned} \tag{26}$$

and

$$z_{H0i} = 0 \quad ; \quad i = 0 \,..\, n \,. \tag{27}$$

$$z_{K0ij} = 0 \quad ; \quad i = 0 \,..\, n \quad ; \quad j = 1 \,..\, m \,. \tag{28}$$

In addition to the specification of the model orders *n*, *m* and *l* which determine the number of elementary hysteresis, creep and superposition operators in the model and the compensator, the maximum of the absolute value of the measured input signal and the maximum and minimum value of the measured output signal must be determined from the measurements. According to (22) the creep eigenvalues $\boldsymbol{a}_K$ follows from the given time resolution T_s. Moreover, during identification (27) and (28) assume the evolution of the hysteretic and creep state from the so-called „virginal“ initial state. Whereas the determination of the infinity norm of the measured input signal and the maximum and minimum value of the measured output signal is easily done by simple min, max and norm operations on the measurement data, the specification of the model orders *n*, *m* and *l* is more heuristic. A practically well suited procedure starts with low model orders and increases them succesively until the error performance index $V(\boldsymbol{w})$ defined below saturates.

The determination of the weights $\mathbf{w}_\mathrm{H}$, $\boldsymbol{w}_K$ and $\boldsymbol{w}_S$' is the aim of the second step and follows from

$$\arg\min\{V(\boldsymbol{w})\} \tag{29}$$

with

$$V(\boldsymbol{w}) = \frac{1}{2}\int_{t_0}^{t_e} E^2[x,y](t)\,\mathrm{d}t = \frac{1}{2}\int_{t_0}^{t_e} (\boldsymbol{w}^T \cdot \boldsymbol{Q}(t))^2\,\mathrm{d}t = \frac{1}{2}\boldsymbol{w}^T \cdot \int_{t_0}^{t_e} \boldsymbol{Q}(t)\boldsymbol{Q}(t)^T\,\mathrm{d}t \cdot \boldsymbol{w}. \tag{30}$$

The problem (29) with (30) describes the least-square minimisation of the generalised error model (23) with

$$\boldsymbol{w} = \begin{pmatrix} \boldsymbol{w}_H \\ \boldsymbol{w}'_S \\ \boldsymbol{w}_K \end{pmatrix} \in \Re^{2n+2l+3} \quad \text{and} \quad \boldsymbol{Q}(t) = \begin{pmatrix} \boldsymbol{H}_{\boldsymbol{r}_H}[x,\boldsymbol{z}_{H0}](t) \\ -\boldsymbol{S}_{\boldsymbol{r}'_S}[y](t) \\ \boldsymbol{K}_{\boldsymbol{r}_K \boldsymbol{a}_K}[x,\boldsymbol{Z}_{K0}](t) \cdot \boldsymbol{i} \end{pmatrix} \in \Re^{2n+2l+3}.$$

To guarantee the existence of the operators H^{-1} and S starting from the operators H and S^{-1} and vice versa and thus the applicability of the transformation mappings (7) - (11) the minimisation problem (29) has to be solved with respect to the linear inequality constraints

$$\boldsymbol{U} \cdot \boldsymbol{w} - \boldsymbol{u} \geq \boldsymbol{o} \tag{31}$$

and

$$\boldsymbol{U} = \begin{pmatrix} \boldsymbol{U}_H & \boldsymbol{O} & \boldsymbol{O} \\ \boldsymbol{O} & \boldsymbol{U}_S & \boldsymbol{O} \\ \boldsymbol{O} & \boldsymbol{O} & \boldsymbol{U}_K \end{pmatrix} \in \Re^{2n+2l+3 \times 2n+2l+3} \quad \text{and} \quad \boldsymbol{u} = \begin{pmatrix} \boldsymbol{u}_H \\ \boldsymbol{u}_S \\ \boldsymbol{u}_K \end{pmatrix} \in \Re^{2n+2l+3}.$$

Due to

$$\frac{1}{2}\int_{t_0}^{t_e} (\boldsymbol{w}^T \cdot \boldsymbol{Q}(t))^2\,\mathrm{d}t \geq 0 \quad \forall \boldsymbol{w} \in \Re^{2n+2l+3} \tag{32}$$

the error performance index $V(\boldsymbol{w})$ is a convex function and thus, the global solution of the optimisation problem (29) - (31) is a convex set [26]. If we assume that Γ models the real system perfectly there exist real values $\boldsymbol{r}_H^*$, $\boldsymbol{w}_H^*$, $\boldsymbol{z}_{H0}^*$, $\boldsymbol{a}_K^*$, $\boldsymbol{r}_K^*$, $\boldsymbol{w}_K^*$, $\boldsymbol{Z}_{K0}^*$, $\boldsymbol{r}_S'^*$, $\boldsymbol{w}_S'^*$ of the generalised error model such that

$$\begin{aligned} E[x,y](t) &= w_{H0}^*\left(\frac{\boldsymbol{w}_H^{*T}}{w_{H0}^*} \cdot \boldsymbol{H}_{\boldsymbol{r}_H^*}[x,\boldsymbol{z}_{H0}^*](t) + \frac{\boldsymbol{w}_K^{*T}}{w_{H0}^*} \cdot \boldsymbol{K}_{\boldsymbol{r}_K^* \boldsymbol{a}_K^*}[x,\boldsymbol{Z}_{K0}^*](t) \cdot \boldsymbol{i} - \frac{\boldsymbol{w}_S'^{*T}}{w_{H0}^*} \cdot \boldsymbol{S}_{\boldsymbol{r}_S'^*}[y](t)\right) \\ &= 0 \quad \forall\, t \ \wedge\ w_{H0}^* \in \Re^+. \end{aligned} \tag{33}$$

Therefore, the expression between the parentheses has to be zero for all times. Thus, the error model is overdeterminded with one degree of freedom and the convex solution set is a one dimensional subspace (a line) in $\Re^{2n+2l+3}$. Therefore, we use one additional equality constraint

$$\boldsymbol{g}^T \cdot \boldsymbol{w} - g = \boldsymbol{o} \tag{34}$$

to cut a single unique solution point from this one dimensional convex solution set. An example for the implementation of the vector $\boldsymbol{g}$ and the scalar g in (34) is directly derived from the condition $w_{H0} = 1$ and is simply given by

$$\boldsymbol{g} = \begin{pmatrix} \boldsymbol{e} \\ \boldsymbol{o} \\ \boldsymbol{o} \end{pmatrix} \in \Re^{2n+2l+3} \quad \text{and} \quad g = 1 \tag{35}$$

with $\boldsymbol{e}^{\mathrm{T}} = (1\ 0\ .\ .\ 0) \in \Re^{n+1}$. Another implementation follows from the requirement that the output range of H+K corresponds to the input range for inifinite slow input signals and results in

$$\boldsymbol{g} = \begin{pmatrix} \|x\|_\infty \boldsymbol{i} - \boldsymbol{r}_H \\ \boldsymbol{o} \\ m\|x\|_\infty \boldsymbol{i} - m\boldsymbol{r}_K \end{pmatrix} \in \Re^{2n+2l+3} \quad \text{and} \quad g = \|x\|_\infty . \tag{36}$$

In the third step the corresponding model Γ and the corresponding compensator Γ^{-1} are generated by the transformation mappings (7) - (9) and (10) - (11), respectively. Fig. 7 shows the whole model and compensator design procedure based on the extended, modified Prandtl-Ishlinskii approach.

As a result, the inequality constraints (31) guarantee the best least-square minimization in that space of the weights which leads to invertible modified Prandtl-Ishlinskii hysteresis and creep operators. Therefore, the invertibility of the modified Prandtl-Ishlinskii hysteresis and creep operator is always guaranteed during the optimisation, and thus the design process for the model or the compensator is in this sense insensitive to unknown measurement errors of input-output data, unknown model errors and unknown model orders.

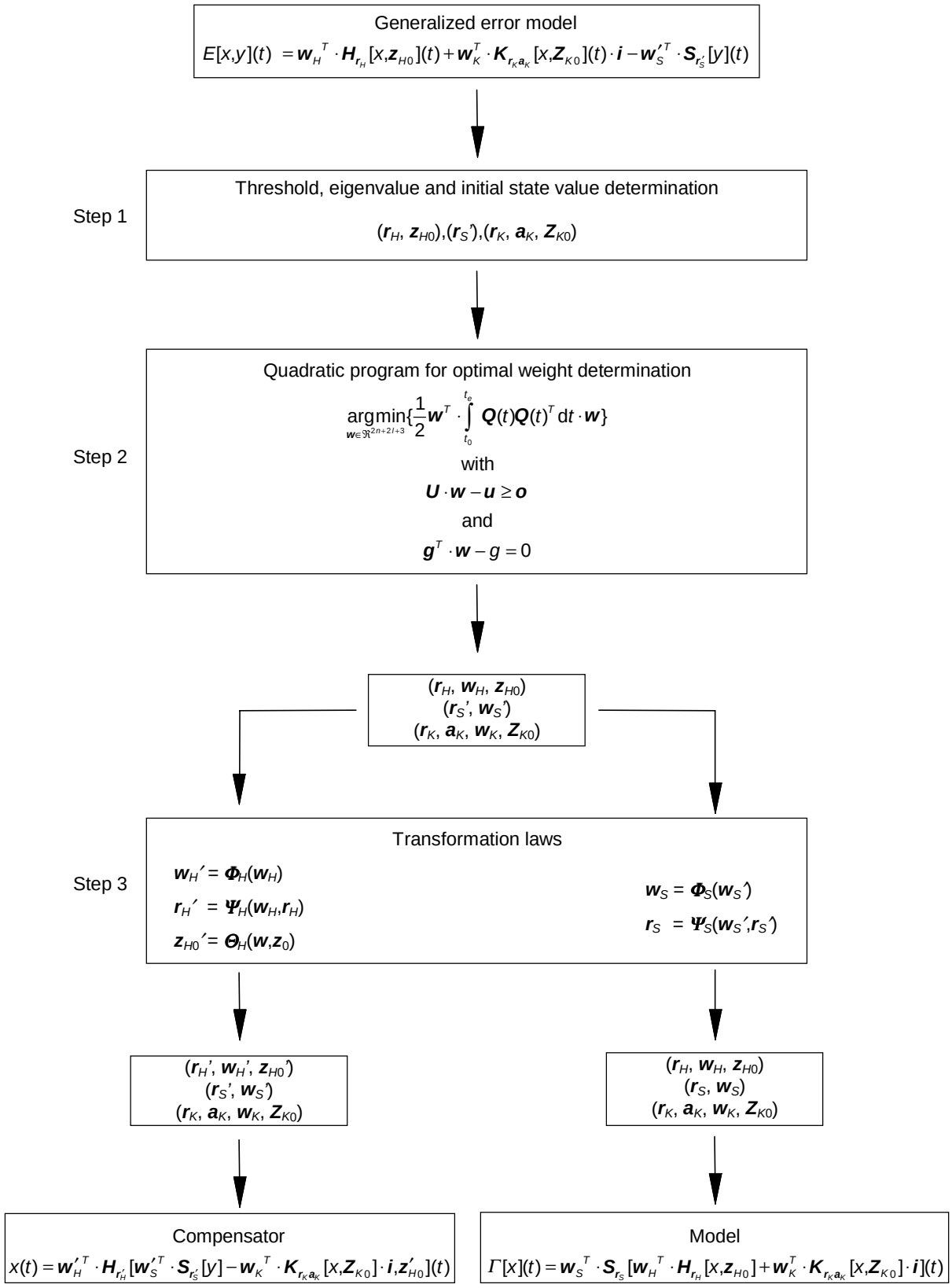

Figure 7. Compensator design procedure.

4 Application to a piezoelectric actuator

In this section the performance of the presented compensator design method for combined complex hysteretic nonlinearities and log(*t*)-type creep dynamics will now be demonstrated by means of the voltage-displacement relationship of a piezoelectric stack transducer. This kind of transducer is used to actuate a micropositioning stage for example in a raster scanning microscope. Fig. 8 illustrates the test and measurement equipment of the experimental part. It consists of a digital signal processor (DSP) which generates the digital driving signal for the piezoelectric actuator. This signal is converted by a 12-bit digital-to-analog converter and amplified by a power amplifier to an analog signal of up to 100 V. The output of the high-voltage power amplifier is measured by an additional voltage measurement circuit and converted to a digital signal by a 12-bit analog-to-digital converter. The displacement of the actuator is measured directly by a high-precision laser-interferometer with a resolution of 5 nm. The signals from the voltage measurement circuit and the interferometer are fed back to the DSP for characterisation, identification and compensation purposes.

Fig. 2 shows the typical voltage-displacement-trajectory of such a piezoelectric device generated by the hysteresis, creep and saturation effects. It is mainly characterized by non-convex increasing branches and asymmetrically closed loops with a counterclockwise orientation. The creep effects cause the displacement signal to change with time although the voltage signal is constant. As a result the voltage-displacement-trajectory in Fig. 2 contains vertical lines which are characteristic of rate-dependent phenomena as they cannot be described by purely rate-independent operators. Therefore, the modeling, identification and compensation of this real combined hysteretic and dynamic nonlinearity cannot be realized with the modified Prandtl-Ishlinskii approach but requires the extensions introduced by the extended modified Prandtl-Ishlinskii approach.

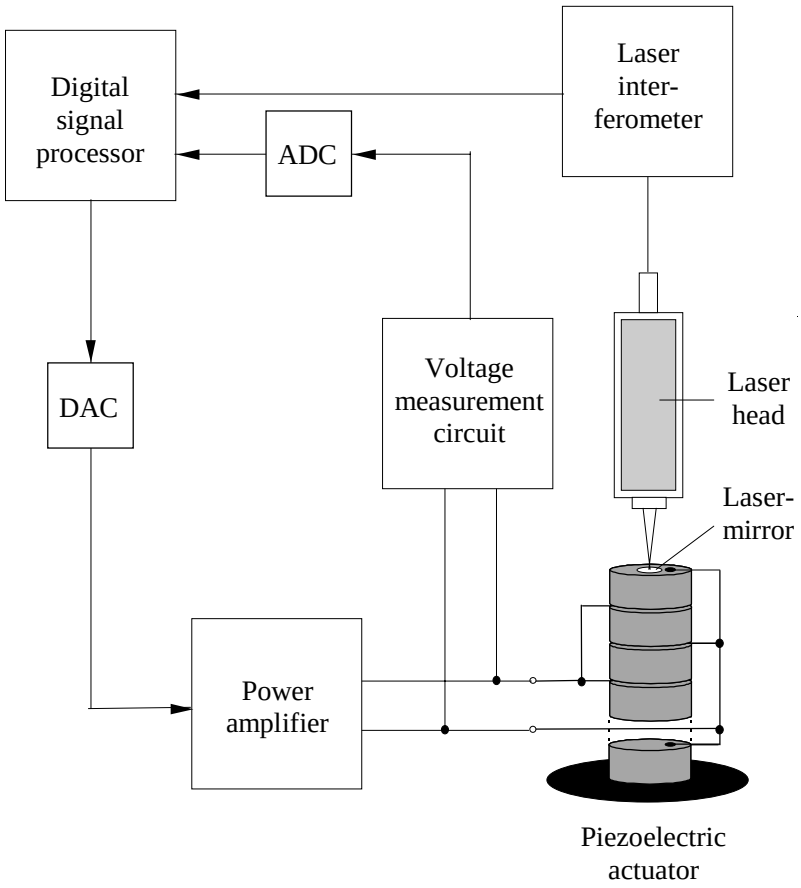

Figure 8. Test and measurement circuit for a piezoelectric actuator.

The lefthand diagram in Fig. 9 shows the measured voltage-displacement-trajectory used for identification. The righthand diagram of Fig. 9 illustrates the modeled voltage-displacement-trajectory of the modified Prandtl-Ishlinskii hysteresis and creep operator for different model orders n, l and m as a result of the identification procedure. The model order $n = 0$, $l = 0$ and $m = 0$ leads to a linear rate-independent operator model, and thus the identification procedure determines the best linear least-square approximation of the real nonlinearity. The nonlinearity error defined by

$$e_r = \frac{\max\limits_{t_0 \le t \le t_e} \{ \left| \Gamma[U](t) - s(t) \right| \}}{\max\limits_{t_0 \le t \le t_e} \{ \left| \Gamma[U](t) \right| \}} \tag{37}$$

amounts in this case up to 14.1 %. Increasing the model order to $n = 6$ and $2l = 6$ and $m = 6$ leads to a much better operator-based approximation of the simultaneously appearing hysteresis, creep and saturation phenomena. The nonlinearity error is in this case reduced to 1.6 % which is nearly one-tenth as great as that for the best linear least-square approximation.

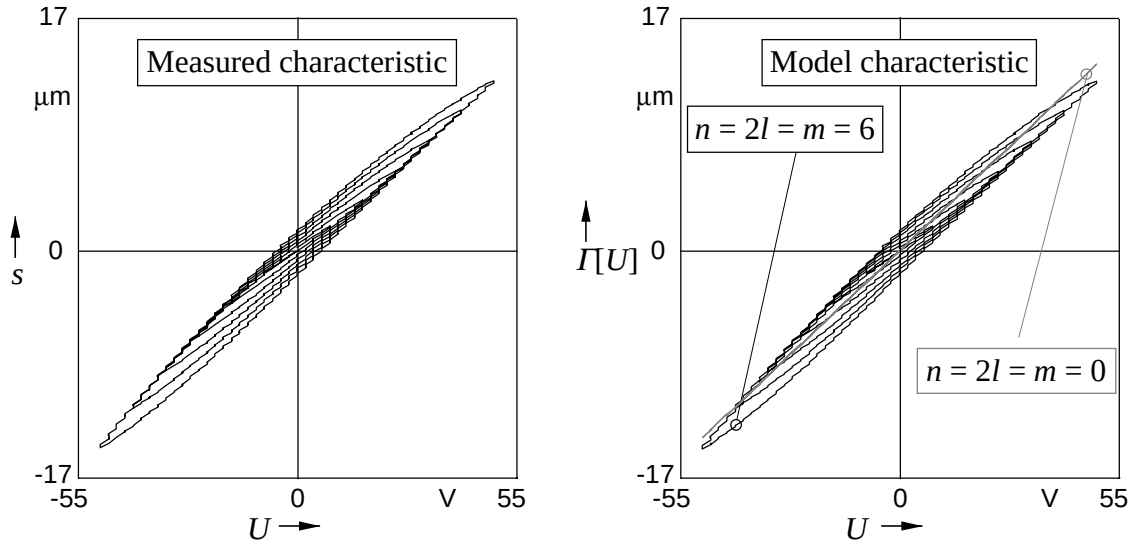

Figure 9. Measured and modeled displacement-voltage relation after identification.

For the compensation of the real complex hysteretic nonlinearity and log(t)-type creep dynamic a feedforward controller is used which is based on the inverse modified threshold-discrete Prandtl-Ishlinskii hysteresis and creep operator Γ^{-1} (Fig. 3). Here $s_c(t)$ is the desired displacement signal value. The inverse modified Prandtl-Ishlinskii hysteresis and creep operator is obtained from the modified Prandtl-Ishlinskii hysteresis and creep operator with the model order of $n = 6$, $2l = 6$ and $m = 6$ using the corresponding transformation laws for the thresholds, weights and initial states. The operator is implemented on a digital signal processor with a sampling rate of up to 1 kHz and a voltage source.

The results of the simultaneous hysteresis, creep and saturation compensation is illustrated in Fig. 10 and Fig. 11. As shown in the upper diagram of Fig. 10 the compensator is driven globally with a low-pass filtered noisy displacement input signal $s_c(t)$ which consists locally of staircase functions. This can be clearly recognized by the enlargement of the part of the given

displacement signal which is encircled in the upper lefthand picture. As a consequence of the inverse filtering the voltage signal $U(t)$ which is shown in the lower middle diagram is properly distorted.

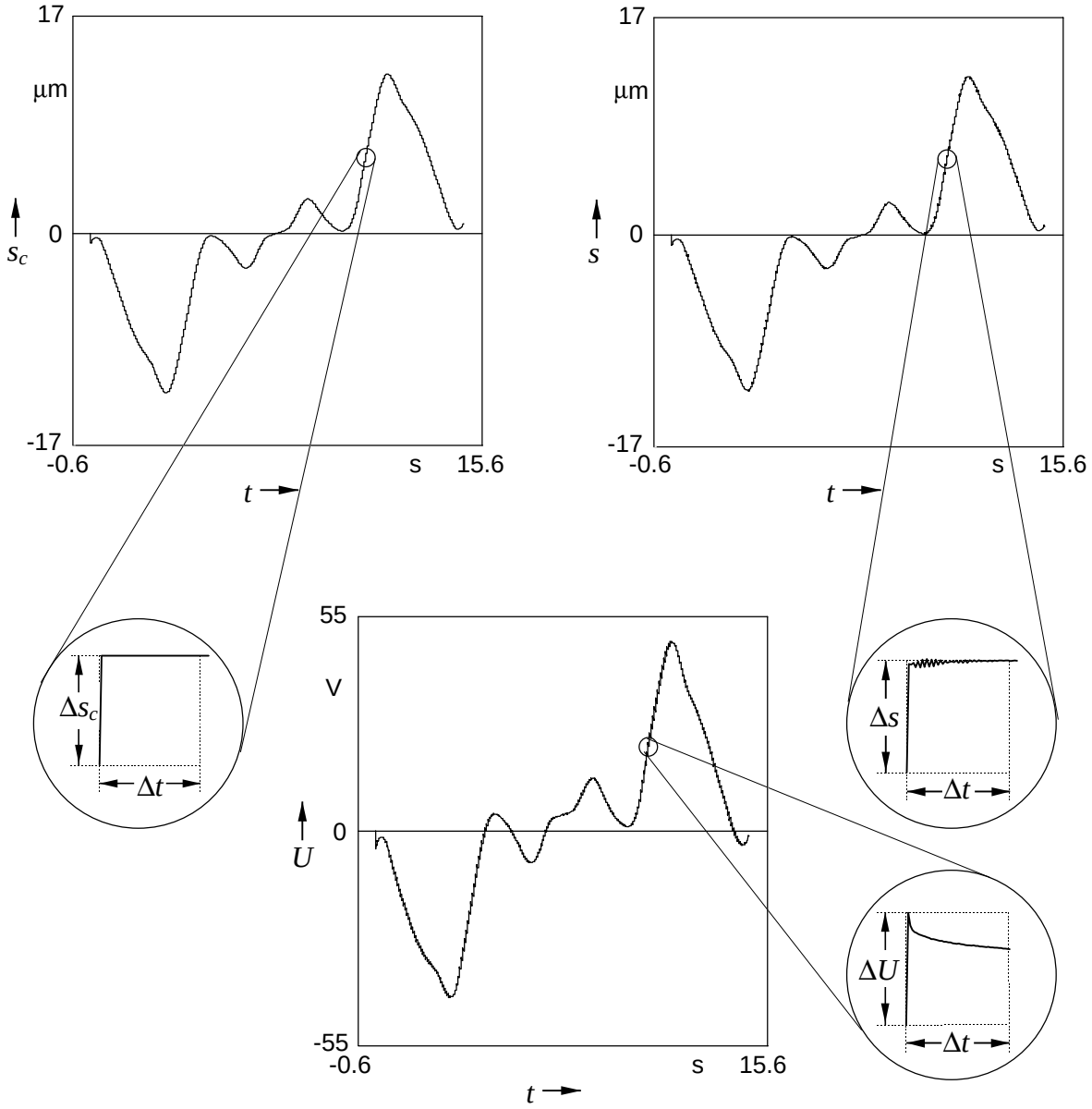

Figure 10. Time signals of the compensation results.

Moreover, due to the incorporation of the Prandtl-Ishlinskii creep operator into the compensator (22) the local staircase functions in the voltage are also disturbed in a manner which counteracts the creep tendency of the piezoelectric actuator as shown in the enlargement of the lower middle diagram of Fig. 2.

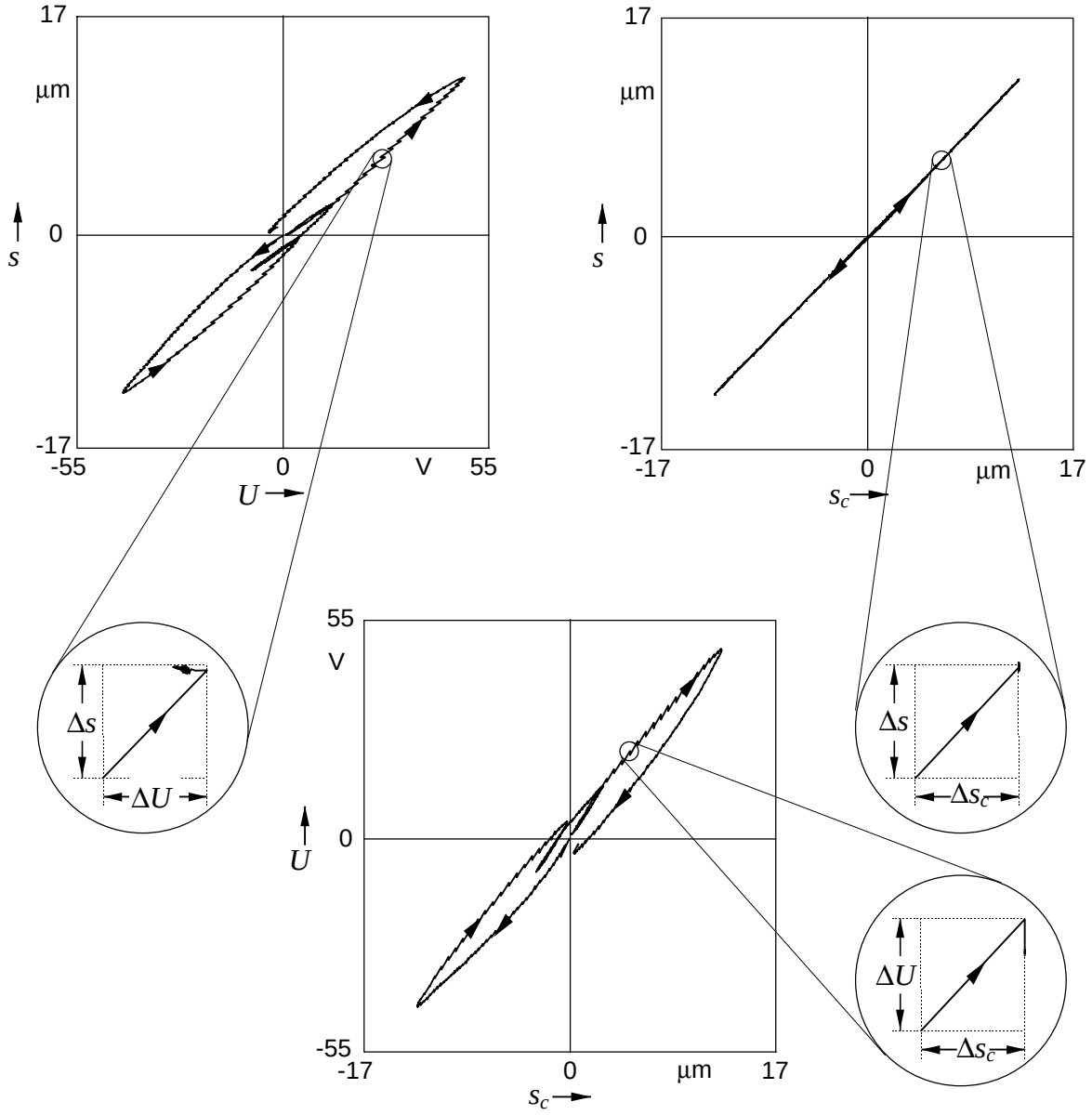

Figure 11. Input-output trajectories of the compensation results.

As a consequence of the inverse feedforward control strategy the measured displacement signal $s(t)$ illustrated in the upper righthand picture of Fig. 10 is nearly identical to the given displacement signal $s_c(t)$. Moreover, enlargement of the upper righthand diagram verifies separately the compensation of creep phenomena via the inverse feedforward control strategy. The local staircase functions of the measured displacement signal are nearly undisturbed in the inverse feedforward controlled case in contrast to the local staircase functions of the conventional feedforward controlled actuator which is illustrated in the enlargement of the upper righthand picture of Fig. 2. The lower middle picture in Fig. 11 shows the voltage

signal from the inverse feedforward controller generated by the given displacement signal in Fig. 10. This trajectory has the inverse branching characteristic of the measured displacement-voltage trajectory shown in the upper lefthand diagram of Fig. 11. As a consequence of the inverse feedforward control strategy the trajectory of the given to measured displacement of the overall system is nearly linear and rate-independent. In this example the control error defined by

$$\frac{\max\limits_{t_0\le t\le t_e}\{\left|s_c(t)-s(t)\right|\}}{\max\limits_{t_0\le t\le t_e}\{\left|s_c(t)\right|\}} \tag{38}$$

will be strongly reduced from 14.1 % without to about 1.7 % with the inverse feedforward control strategy.

5 Conclusions

The main contribution of this paper is to extend the modified Prandtl-Ishlinskii approach for the modeling, identification and compensation of complex hysteretic nonlinearities to a so-called extended modified Prandtl-Ishlinskii approach for combining complex hysteretic nonlinearities and complex log(*t*)-type creep dynamics. These nonlinear properties are typical for the technologically important piezoelectric actuators. For this purpose in the modified Prandtl-Ishlinskii hysteresis operator, defined by the serial combination of a conventional Prandtl-Ishlinskii hysteresis operator and a memory-free nonlinearity, the conventional Prandtl-Ishlinskii hysteresis operator is replaced by the parallel combination of a conventional Prandtl-Ishlinskii hysteresis operator and a so-called Prandtl-Ishlinskii creep operator. The Prandtl-Ishlinskii creep operator used converges to the conventional Prandtl-Ishlinskii hysteresis operator for infinitely slow input signals and thus can be understood as a consistent dynamic extension of Prandtl-Ishlinskii-type complex hysteretic nonlinearities. Based on this modeling method, a robust compensator design procedure for such complex hysteretic and

creep nonlinearities is developed. Finally, the compensator design method is used to generate an inverse feedforward controller for a piezoelectric actuator. In comparison to the conventionally controlled piezoelectric actuator the nonlinearity error of the inverse controlled piezoelectric actuator is lowered from about 14 % to about 1.7 %.

In future works the extended modified Prandtl-Ishlinskii approach to modeling, identification and compensation of complex hysteretic nonlinearities and log(*t*)-type creep dynamics will be developed further to self-learning and adaptive observer and inverse feedforward controller structures.

Acknowledgement

The results of this work are obtained within the project "Investigations of Extended Preisach Models for Solid-State Actuators". The author thanks the Deutsche Forschungsgemeinschaft (DFG) for the financial support of this work, Prof. Dr. Hartmut Janocha from the Laboratory for Process Automation (LPA) at Saarland University for the non-financial support of this project and Dr. Pavel Krejci from the Dept. of Evolution Differential Equations at the Mathematical Institute of the Academy of Sciences in Prague for his contributions to the mathematical aspects of this work.

References

[1] A. Visintin, *Differential Models of Hysteresis*. (Berlin-Heidelberg: Springer, 1994).

[2] E. Madelung, Über Magnetisierung durch schnellverlaufende Ströme und die Wirkungsweise des Rutherford-Marconischen Magnetdetektors. *Ann. der Physik, 17* 1905, 861-890.

[3] I.D. Mayergoyz, *Mathematical Models of Hysteresis*. (Berlin-Heidelberg-New York: Springer, 1991).

[4] M. Brokate & J. Sprekels, *Hysteresis and Phase Transitions*. (New York-Berlin-Heidelberg: Springer, 1996).

[5] M.A. Krasnosel'skii & A.V. Pokrovskii, *Systems with Hysteresis* (Berlin: Springer, 1989).

[6] G.V. Webb, D.C. Lagoudas & A.J. Kurdila, Hysteresis Modeling of SMA Actuators for Control Applications, *Journal of Intelligent Material Systems and Structures*, *9*, 1998, 432-448.

[7] K. Kuhnen & H. Janocha, Inverse feedforward controller for complex hysteretic nonlinearities in smart material systems, *Control and Intelligent Systems, 29*(3), 2001, 74-83.

[8] H.T. Banks & R.C. Smith, Hysteresis Modeling in Smart Material Systems, *Journal of Applied Mechanics and Engineering, 5*(1), 2000, 31-45.

[9] O. M. El Rifai & K. Youcef-Toumi, Creep in Piezoelectric Scanners of Atomic Force Microscopes, *Proc. of the American Control Conf.*, Anchorage, 2002, 3777-3782.

[10] P. Ge & M. Jouaneh, Generalized Preisach Model for Hysteresis Nonlinearity of Piezoceramic Actuators, *Journal of Precision Engineering, 20*, 1997, 99-111.

[11] J. Schäfer & H. Janocha, Compensation of Hysteresis in solid-state Actuators, *Sensors and Actuators, Physical A, 49*, 1995, 97-102.

[12] M. Dimmler, U. Holmberg & R. Longchamp, Hysteresis Compensation of Piezo Actuators, *Proc. of the European Control Conf.*, Karlsruhe, 1999, Rubicom GmbH (CD-ROM).

[13] M. Goldfarb & N. Celanovic, Modeling Piezoelectric Stack Actuators for Control of Micromanipulation, *IEEE Control Systems, 17*(3), 1997, 69-79.

[14] K. Kuhnen & H. Janocha, Adaptive Inverse Control of Piezoelectric Actuators with Hysteresis Operators, *Proc. of the European Control Conf.*, Karlsruhe, 1999, Rubicom GmbH (CD-ROM).

[15] K. Kuhnen, Modeling, Identification and Compensation of complex hysteretic Nonlinearities - A modified Prandtl-Ishlinskii approach, *European Journal of Control, 9*(4), 2003, 407-418.

[16] G. Tao & P.V. Kokotovic, Adaptive Control of Plants with Unknown Hysteresis. *IEEE Transactions on Automatic Control, 40*(2), 1995, 200-212.

[17] C.S. Su, Y. Stepanenko, J. Svoboda & T.P. Leung, Robust Adaptive Control of a Class of Nonlinear Systems with Unknown Backlash-Like Hysteresis. *IEEE Transaction on Automatic Control, 45*(12), 2000, 2427-2432.

[18] J. Lemaitre & J.L. Chaboche, *Mechanics of solid materials.* (New York:: Cambridge University Press, 1990).

[19] H. Kortendieck, *Entwicklung und Erprobung von Modellen zur Kriech- und Hysteresiskorrektur*. Düsseldorf: VDI, 1993.

[20] K. Kuhnen & H. Janocha, Compensation of Creep and Hysteresis Effects of Piezoelectric Actuators with Inverse Systems, *Proc. of the 6th Int. Conf. on New Actuators*, Bremen, 1998, 309-312.

[21] P. Krejcí & K. Kuhnen, Inverse Control of Systems with Hysteresis and Creep, *IEE Proc.-Control Theory Appl., 148*(3), 2001, 185-192.

[22] H. Janocha & K. Kuhnen, Real-time Compensation of Hysteresis and Creep in Piezoelectric Actuators, *Sensors & Actuators Physical A, 79*, 2000, 83-89.

[23] P. Haupt, *Continuum Mechanics and Theory of Materials*, (Berlin-Heidelberg-New York: Springer, 2002).

[24] P. Krejci, *Hysteresis, Convexity and Dissipation in Hyperbolic Equations*. (Tokyo: Gakuto Int. Series Math. Sci. & Appl. Vol. 8, Gakotosho, 1996).

[25] K. Kuhnen, *Inverse Steuerung piezoelektrischer Aktoren mit Hysterese-, Kriech- und Superpositionsoperatoren.* Doctoral Thesis, Saarland University, (Aachen: Shaker, 2001).

[26] M. Papageorgiou, *Optimierung*. (München: Oldenbourg, 1991).

[27] G. Tao & F. Lewis (Ed), *Adaptive Control of Nonsmooth Dynamic Systems*. (London: Springer, 2001).

Biographie

Klaus Kuhnen, born in 1967, received the Dipl.-Ing. degree in electrical engineering at the University of Saarland in 1994. As following graduation, he has been working there as a scientific collaborator at the Laboratory for Process Automation (LPA) in the fields of solid-state actuators and control of systems with hysteresis and creep. Since 2000 he works as scientific assistant at the Laboratory for Process Automation (LPA) in the fields of self-sensing solid-state actuators, active vibration damping with active material systems and adaptive identification and compensation with convex constraints. He received the Dr.-Ing. degree in engineering sciences at the University of Saarland in 2001. His research interests are in the mechatronic systems with active materials, the control of systems with hysteresis and creep and adaptive control theory.